

Exploring Text-to-Motion Generation with Human Preference

Jenny Sheng^{*1} Matthieu Lin^{*1} Andrew Zhao¹ Kevin Pruvost¹ Yu-Hui Wen²
 Yangguang Li³ Gao Huang¹ Yong-Jin Liu¹

¹ Tsinghua University ² Beijing Jiaotong University ³ Shanghai AI Lab

{cqq22, yh-lin21, zqc21, pkw23}@mails.tsinghua.edu.cn, yhw1@bjtu.edu.cn,
 liyangguang256@gmail.com, {liuyongjin, gaohuang}@tsinghua.edu.cn

Abstract

This paper presents an exploration of preference learning in text-to-motion generation. We find that current improvements in text-to-motion generation still rely on datasets requiring expert labelers with motion capture systems. Instead, learning from human preference data does not require motion capture systems; a labeler with no expertise simply compares two generated motions. This is particularly efficient because evaluating the model’s output is easier than gathering the motion that performs a desired task (e.g. backflip). To pioneer the exploration of this paradigm, we annotate 3,528 preference pairs generated by MotionGPT, marking the first effort to investigate various algorithms for learning from preference data. In particular, our exploration highlights important design choices when using preference data. Additionally, our experimental results show that preference learning has the potential to greatly improve current text-to-motion generative models. Our code and dataset will be publicly available to further facilitate research in this area.

1. Introduction

Human text-to-motion generation [2, 6, 12, 15, 19, 27, 30, 33, 44, 47–51] is a profoundly pertinent task with extensive applicability in computer animation, movie production, gaming, and robotics. However, current text-to-motion generation research relies on relatively modest datasets compared to language tasks, as expert labelers with specialized motion capture systems are costly and labor-intensive. Due to the lack of large-scale data, these models are poorly aligned with the text prompt [19, 47, 51].

Learning from preference data [26, 32, 54] has emerged as a powerful novel training paradigm in cases where evaluation proves simpler than generation. With a simple data

collection pipeline where layman labelers compare two motion sequences, preference data gives us extremely cost-effective labels to improve text-to-motion generation models without expert labelers.

While learning from preference data has excelled in domains abundant with datasets, particularly in language tasks benefiting from ample and high-quality data, its application in fields constrained by limited, multi-modal data presents a unique challenge. The current landscape of learning from preference data is rife with intricate engineering details and subtle design choices, often concealed within implementations and validated solely through empirical experimentation [26, 36, 40, 53]. Yet, there are currently no existing motion datasets tailored for exploring preference learning techniques. As a result, initiatives to extend preference learning to these low-data, multi-modal setups remain absent, for they lack empirical evidence to substantiate the intricate design decisions pivotal for applying preference learning in text-to-motion generation. This absence underscores an intriguing gap in our understanding and presents an exciting opportunity to investigate how preference learning performs in text-to-motion generation tasks where data is scarce.

Previous endeavors address data scarcity by aligning to large language models’ (LLMs) rich representation [19, 51]. While this approach transfers some of the compositional structure of language, it nonetheless requires a large dataset of text and motion pairs, failing to circumvent the data issue. Other methods resort to pseudo-labeled data [21] to offset the dearth of large-scale datasets in text-to-motion generation. However, such approaches often introduce noisy learning signals that may amplify problems, such as perceptually unrealistic motions. Alternatives involve injecting noise into existing labels and learning from the resulting ranked generations [41]. Nonetheless, this approach neglects training on the actual policy distribution, leading to a distributional gap wherein the reward model is not trained to supervise the actual policy.

We classify existing methodologies according to the ap-

^{*} These authors contributed equally to this work.

proximations employed to represent the preference distribution. In particular, current methods make one or both of the following approximations. First, they assume that pairwise preferences can be substituted by a scalar reward. In particular, they employ the Bradley-Terry probabilistic model [5] to connect scalar rewards to preferences. Second, they assume that a reward model trained with the Bradley-Terry model generalizes so that it can accurately evaluate samples from the policy. Notably, it uses reinforcement learning (RL) to finetune against the reward model. While reinforcement learning from human feedback (RLHF) makes both assumptions, direct preference optimization (DPO) bypasses the RL step. RLHF [26] trains a reward model in a supervised way on the preference data, then finetunes the policy by optimizing against that reward model using reinforcement learning. In contrast, DPO [28] directly finetunes the preference data in a supervised manner using cross-entropy. DPO is a simpler algorithm, yet it lacks a crucial element found in online RL-based algorithms: exploration. By training a reward model, we can generalize to unseen samples. Accordingly, our policy can generate samples outside of the preference dataset (*i.e.*, exploration). In other words, RLHF allows us to get a training signal where the reward model generalizes via trial and error, thereby acquiring more information. Conversely, DPO is limited to two points within the data, optimizing to maximize one while minimizing the other.

We explore the aforementioned methods along their variants, and summarize our contribution as follows:

1. We annotate 3,528 preference pairs generated by MotionGPT [19]. Additionally, we provide a degree of preference for each choice.
2. We are the first to demonstrate effective implementation of preference learning on text-to-motion generation models. Our results show that labelers exhibit a significant preference for outputs from MotionGPT when trained with preference data, a trend that persists across temperatures ranging from 1.0 to 2.0.
3. Our findings indicate that the scarcity of large-scale text-motion pairs leads to a propensity for the reward model to overfit. Consequently, this overfitting hampers its ability to accurately assess outputs generated by MotionGPT. In light of this, we propose the adoption of DPO, a method that circumvents the optimization over a reward model, thereby avoiding reward hacking.
4. We find that labels characterized by a pronounced degree of preference significantly contribute to the observed enhancement in R-precision. This suggests that the differential quality of preference annotations plays a pivotal role in driving the efficacy of the model.

We organize this paper as follows. We present related works in Sec. 2. Our work finetunes upon MotionGPT [19], which we present in Sec. 3. We detail the implementation of our

data collection pipeline alongside specific design details for RLHF and DPO in Sec. 4. Experimental results in Sec. 5 illustrate our key design choices. Finally, Sec. 6 contains a summary of our findings and discusses future work.

2. Related Works

2.1. Autoregressive Text-to-Motion Generation

Numerous text-to-motion generation methods leverage diffusion models to generate motion sequences [2, 6, 27, 30, 33, 44, 48–50]. However, human motion inherently exhibits semantic connections and is frequently interpreted as a form of body language, conveying meaning and intent. Following this observation, several works have explored treating motion as a form of language and using the generative transformer framework to model human motion, akin to the current methods for modeling language [19, 51]. This approach involves converting motions into discrete tokens using vector quantization (VQ) [37] and inputting them into an autoregressive model to generate a sequence of motion tokens in a unidirectional manner [12, 15, 47]. Subsequent works also leverage pretrained LLMs such as T5 [29] and LLaMA [35] to conduct comprehensive language modeling on both textual and motion inputs by expanding the existing LLM vocabulary with motion tokens [19, 51]. In this work, we build upon autoregressive Transformers [38], which have tractable log-likelihood, an essential element for preference learning methods.

2.2. Learning from Human Preferences

The initial exploration of learning from human preferences begins in the RL community with training agents to play Atari [8, 17]. Further exploration occurs in the domain of language modeling, where human feedback is incorporated to improve specific tasks like summarization [32, 54] and using external information to increase accuracy [23, 24, 34].

Building upon the aforementioned works, Ouyang et al. [26] shows that a blend of instruction fine-tuning and RLHF effectively addresses issues related to factuality, toxicity, and helpfulness, which cannot be resolved solely by increasing the scale of LLMs. Leveraging the proposed RLHF framework, numerous LLMs [11, 25, 36] incorporate the RLHF phase into their training process to mitigate potential model-related harm. The research community is also increasingly exploring other human preference learning methods [4, 7, 10, 13, 28, 31, 43, 52] that mitigate certain issues associated with RLHF, such as reward hacking [28], requirements for preference pairs [10], and complex hyperparameter tuning [43].

Motivated by the very successful application of preference learning in language modeling, preference learning is now increasingly being applied to other domains. For example, Lee et al. [20] and Wu et al. [42] apply RLHF to text-

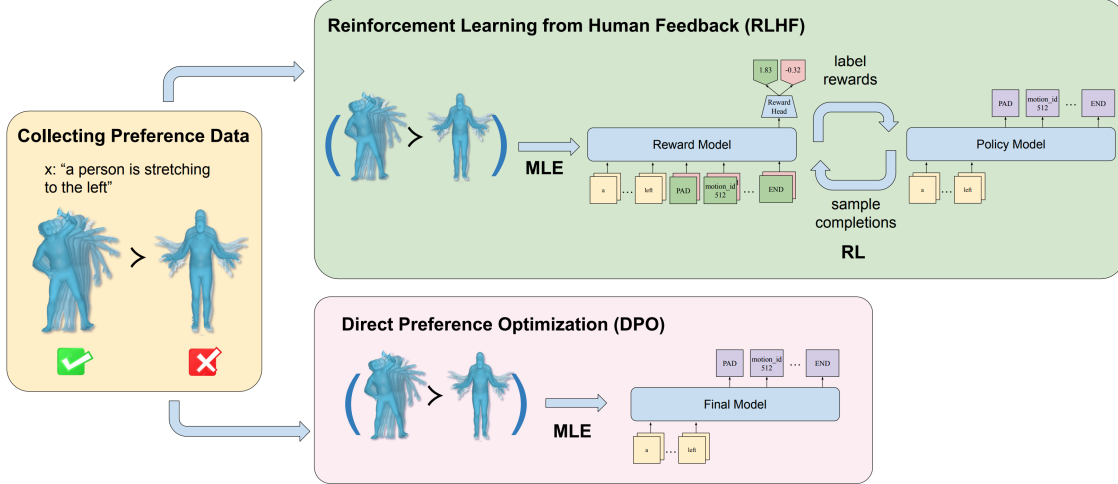


Figure 1. **Text-to-Motion Generation with Human Preference.** We gather preferences over generated completion (*i.e.*, motion) pairs and use them to finetune MotionGPT. In preference learning, the likelihood of preferred completion is increased while that of dispreferred completion is decreased. We explore two types of practical algorithms for preference learning. First, RLHF trains in an online manner; it trains a reward model on the data and uses it to perform RL on MotionGPT. Second, DPO trains in an offline manner with supervised learning; it directly performs MLE on the data. The online/offline aspect is related to whether or not the policy performs exploration, *i.e.*, training on completions outside of the preference dataset.

to-image synthesis models, and Cideron et al. [9] utilizes RLHF for music generation. Despite its promising potential, the research community has yet to witness its application in text-to-motion generation or scenarios with limited data resources. This untapped area of exploration represents a significant opportunity to advance our understanding of how these methods can be leveraged effectively in contexts where data availability is constrained, thereby opening new avenues for research and innovation in text-to-motion generation and related disciplines. Its application is particularly relevant to text-to-motion generation, where evaluating two motions is considerably easier than collecting motion data with costly motion capture systems.

3. Preliminary

This section reviews MotionGPT [19], the supervised baseline upon which we use preference learning to finetune. Additionally, we present our data collection pipeline that uses sample pairs generated by MotionGPT.

MotionGPT. Formulating text-to-motion generation as a sequence modeling problem allows building upon LLMs. This holds the premise of transferring language’s compositional semantic structure to other modalities, thereby achieving off-the-shelf, out-of-distribution generalization. Casting text-to-motion generation as a sequence modeling problem requires discretizing the motion modality into tokens, as done by MotionGPT. The discretization process is akin to the tokenization of strings to tokens in language processing. In particular, they first map the motion dataset

into a set of discrete tokens using a vector quantized variational autoencoder [37]. Then, a pretrained LLM is finetuned to generate corresponding motion tokens from the textual prompt. Thus, MotionGPT is an autoregressive model where the completions are motion tokens instead of word tokens.

Collecting preference data. As shown in Fig. 2, we build a labeling platform with Gradio [1], where labelers are presented with two different completions from a prompt. The labelers are tasked to read each prompt and choose the motion that corresponds best to the prompt. Additionally, the labelers provide a degree of preference for their choice, choosing from “Negligibly better/unsure,” “Slightly better,” “Better,” and “Much better.” We find that MotionGPT produces samples that are hard to distinguish when given a prompt from the training dataset, thus indicating signs of overfitting. Accordingly, we prompt gpt-3.5-turbo-0125 [25] to generate a new set of prompts similar to those in the training set. For each prompt, we sample two completions from MotionGPT by using different seeds and a temperature of 1.2 to promote diversity. Our labelers are six graduate students in computer science. We find that it is important to recruit labelers with prior exposure to generative models. Our initial exploration indicates that labelers with similar prior experience is crucial for achieving a high level of agreement. Quantitatively, we obtain an agreement of 84% on average (42 samples out of 50 samples). Note that in some cases, the model completely fails to generate perceptually realistic motion for both seeds. Accordingly, the labelers mark them as “Skipped.” Upon inspection, we

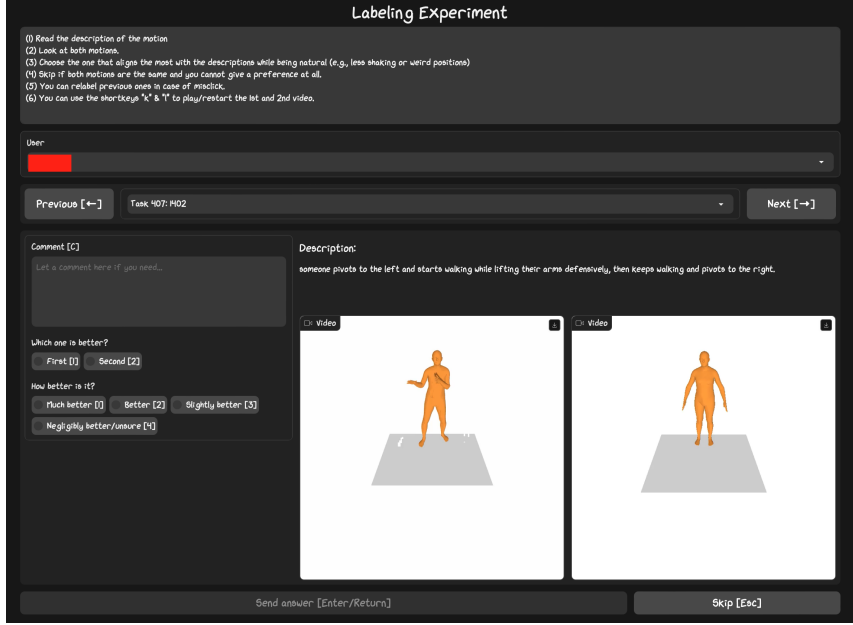


Figure 2. Screenshot of the Gradio interface for data labeling.

find that two cases often occur: (1) one generation is “Much better,” with one seed failing to generate reasonable motion while the other seed partially achieving the motion, (2) the motion pair is “Skipped,” with both seeds failing to generate reasonable motions. The resulting dataset contains 3,528 annotated pairs, with 996 pairs labeled as “Much better,” 607 pairs labeled as “Better,” 497 pairs labeled as “Slightly better,” and 116 pairs labeled as “Negligibly better/unsure.” Additionally, there are 1312 examples labeled as “Skipped.” We randomly select 10% of the total dataset to be the test dataset, with the remaining data designated for training.

4. Method

We organize this section as follows. Sec. 4.1 presents the objective function in preference learning. Then, we present practical algorithms for optimizing this objective: RLHF based on reinforcement learning in Sec. 4.2 and DPO based on supervised learning in Sec. 4.3.

Notations. Denote sequences of tokens in bold where $\mathbf{x} = (x_1, x_2, \dots)$ is a textual prompt and $\mathbf{y} = (y_1, y_2, \dots)$ is a completion, *i.e.* a generated motion sequence.

4.1. Preference Learning

We formulate the objective function for learning from human preference data as in Azar et al. [3]. Intuitively, given prompts $\mathbf{x} \sim \rho$, it involves maximizing the probability that our policy generates completion $\mathbf{y} \sim \pi_\theta(\cdot | \mathbf{x})$ preferred over the original model $\mathbf{y}' \sim \mu(\cdot | \mathbf{x})$, under the constraint that our distribution stays close to that of some reference policy π_{ref} to prevent over-optimization. In most cases, μ

and π_{ref} are the same model, but it is not uncommon to initialize them differently. In formulae, we maximize the following objective in preference learning:

$$J(\theta) = \mathbb{E}_{\substack{\mathbf{x} \sim \rho \\ \mathbf{y} \sim \pi_\theta(\cdot | \mathbf{x}) \\ \mathbf{y}' \sim \mu(\cdot | \mathbf{x})}} \left[\Psi(p^*(\mathbf{y} \succ \mathbf{y}' | \mathbf{x})) \right] - \beta \text{KL}(\pi_\theta || \pi_{\text{ref}}), \quad (1)$$

where $p^*(\mathbf{y} \succ \mathbf{y}' | \mathbf{x})$ is the probability of \mathbf{y} being preferred to \mathbf{y}' knowing the prompt \mathbf{x} . First, $\Psi : [0, 1] \rightarrow \mathbb{R}$ is a non-decreasing function that maps probabilities to real scalars. Intuitively, such mapping allows a non-linear mapping of preference probabilities to scores, yielding a reward maximization objective. Second, the KL term is a *per-token* KL that regularizes training in two ways. In formulae, the KL term can be rewritten as

$$\text{KL}(\pi_\theta || \pi_{\text{ref}}) = \underbrace{\mathbb{H}[\pi_\theta, \pi_{\text{ref}}]}_{\text{cross entropy}} - \underbrace{\mathbb{H}[\pi_\theta]}_{\text{entropy}}. \quad (2)$$

The cross-entropy term acts as a regularizer that prevents deviating too far from the reference model. It helps against hacking the objective function. The entropy term promotes exploration. It prevents the model from mode collapse, where the policy outputs sequences with high scores but low diversity. We want to maximize the score while maintaining a low KL divergence with high entropy.

As illustrated in Fig. 1, there are two types of algorithms for solving the optimization problem in Eq. 1. In both algorithms, the underlying assumption is that the probability $p^*(\mathbf{y} \succ \mathbf{y}' | \mathbf{x})$ is implemented as the Bradley-Terry

probabilistic model [5]. Accordingly, we have $\Psi(q) = \log(q/(1-q))$. In practice, the Bradley-Terry model is implemented as a sigmoid function σ :

$$p^*(\mathbf{y} \succ \mathbf{y}' | \mathbf{x}) = \sigma(r(\mathbf{x}, \mathbf{y}) - r(\mathbf{x}, \mathbf{y}')), \quad (3)$$

thus the probability of preferring a completion depends *exponentially* on the value of a latent scalar.

Next, to understand the difficulties induced by the Bradley-Terry model in Eq. 3, we turn to the analytical optimal solution to the objective in Eq. 1:

$$\pi_{\theta^*}(\mathbf{y} | \mathbf{x}) = \frac{1}{Z(\mathbf{x})} \pi_{\text{ref}}(\mathbf{y} | \mathbf{x}) \exp(\beta^{-1} r(\mathbf{x}, \mathbf{y})). \quad (4)$$

As detailed in Eq. 4, the probability we assign to a particular response is the product of the probability that our reference model assigns to that response and the exponentiated latent scalar. The problem is that if $p^*(\mathbf{y} \succ \mathbf{y}' | \mathbf{x}) = 1$, it means that $r(\mathbf{x}, \mathbf{y}) \rightarrow \infty$. As a result, the strength of the KL divergence β vanishes, and the model is *prone to overfitting*.

We just observed that the current implementation of Ψ assumes that pairwise preferences can be substituted with pointwise rewards. Next, we present RLHF in Sec. 4.2 and DPO in Sec. 4.3, the two most commonly taken approaches in LLM alignment. Notably, these two algorithms differ in being online or offline. RLHF is online because it trains with RL, *i.e.* there is exploration. At each step, a policy generates samples and receives feedback from a reward model. In particular, it assumes that a reward model trained on pointwise rewards generalizes so that it can accurately evaluate samples from the policy. DPO, on the other hand, is offline because it operates without continuous interaction with the environment; instead, it optimizes based on pre-determined data points.

4.2. RL with Human Feedback

RLHF is a bi-level optimization problem involving learning a reward model $r_\psi(\mathbf{x}, \mathbf{y})$ in a supervised manner, with a cross-entropy loss between the distribution of preference and the Bradley-Terry model. Given a dataset of preferences $\mathcal{D} = \{\mathbf{x}, \mathbf{y}_w, \mathbf{y}_l\}$, where \mathbf{y}_w is the chosen sample, \mathbf{y}_l is the rejected sample, and \mathbf{x} is the input prompt, we minimize the following cross-entropy loss:

$$-\mathbb{E}_{(\mathbf{x}, \mathbf{y}_w, \mathbf{y}_l) \sim \mathcal{D}} [\log \sigma(r_\psi(\mathbf{x}, \mathbf{y}_w) - r_\psi(\mathbf{x}, \mathbf{y}_l))]. \quad (5)$$

Then, we define Eq. 1 in terms of the trained reward model $r_\psi(\mathbf{x}, \mathbf{y})$ as an approximation of $\Psi(\cdot)$:

$$J(\theta) = \mathbb{E}_{\mathbf{x} \sim \rho, \mathbf{y} \sim \pi_\theta} [r_\psi(\mathbf{x}, \mathbf{y})] - \beta \mathbb{KL}(\pi_\theta \| \pi_{\text{ref}}), \quad (6)$$

and optimize our policy π_θ against that reward model. The objective requires maximizing a reward function based on a distribution induced by the policy π_θ . Thus, evaluating this

expected value requires sampling from our policy. We use policy gradient to backpropagate through random samples from our policy.

The objective in Eq. 6 is implemented with the Bradley-Terry model, thus is prone to overfitting. Accordingly, we want to regularize the reward model to avoid $r_\psi(\mathbf{x}, \mathbf{y}) \rightarrow \infty$ when $p^*(\mathbf{y} \succ \mathbf{y}' | \mathbf{x}) = \{0, 1\}$. As mentioned in Sec. 4.1, when $r_\psi(\mathbf{x}, \mathbf{y}) \rightarrow \infty$, the KL regularization β vanishes. In particular, we find that the scarce dataset in text-to-motion generation leads to overfitting: the reward model’s training loss converges to 0 while the validation loss increases.

During policy optimization, due to the overfitted reward, the policy tries to hack the reward function and selects tokens that are very improbable under the reference model. As a result, the KL divergence explodes, and so does the reward. Accordingly, the value network is also affected by these sudden spikes. We experimentally find it hard to prevent these spikes. In particular, we found that removing dropout is essential to diminishing the spikes. Surprisingly, we observe that preventing these spikes is not related to better performance as evaluated by FID and R-precision. Overall, we find RLHF particularly difficult to tune in our setup, owing to the instabilities resulting from a reward model’s inability to evaluate samples accurately. Instead, we recommend using DPO, which we present next.

4.3. Direct Preference Optimization

In DPO, we skip the step of learning a reward model and directly train our policy on the preference data. In particular, we rewrite Eq. 4 the reward function as a function of the optimal policy π_{θ^*} to Eq. 1:

$$r(\mathbf{x}, \mathbf{y}) = \beta \log \frac{\pi_{\theta^*}(\mathbf{y} | \mathbf{x})}{\pi_{\text{ref}}(\mathbf{y} | \mathbf{x})} + \beta \log Z(\mathbf{x}), \quad (7)$$

where $Z(\mathbf{x})$ is the normalization constant. Originally in RLHF, we had a loss function on the reward functions to turn our preference data into a reward function. We use Eq. 7 to turn the loss function over reward functions in Eq. 5 into a loss function on policies. In particular, we write Eq. 7 in terms of our current policy π_θ instead of the optimal policy π_{θ^*} , which we denote as $\hat{r}_\theta(\mathbf{x}, \mathbf{y})$:

$$\hat{r}_\theta(\mathbf{x}, \mathbf{y}) = \beta \log \frac{\pi_\theta(\mathbf{y} | \mathbf{x})}{\pi_{\text{ref}}(\mathbf{y} | \mathbf{x})} + \beta \log Z(\mathbf{x}). \quad (8)$$

Intuitively, the logarithmic ratio yields a positive value when the policy assigns a higher probability to the response compared to the reference model, indicating a preference. Conversely, it results in a negative value when the policy deems the response less probable than what the reference model suggests, signifying a lesser preference. Then, the objective for DPO is:

$$-\mathbb{E}_{(\mathbf{x}, \mathbf{y}_w, \mathbf{y}_l) \sim \mathcal{D}} [\log \sigma(\hat{r}_\theta(\mathbf{x}, \mathbf{y}_w) - \hat{r}_\theta(\mathbf{x}, \mathbf{y}_l))]. \quad (9)$$

Method	Alignment				Quality		
	Top-1↑	Top-2↑	Top-3↑	MM Dist↓	MModality↑	FID↓	Diversity→
Real motion	0.494±0.002	0.677±0.002	0.769±0.002	3.224±0.008	-	0.002±0.000	9.463±0.073
MotionGPT [19]	0.405±0.002	0.567±0.002	0.658±0.002	4.027±0.011	3.495±0.162	0.178±0.008	9.393±0.086
RLHF [26]	0.415±0.002	0.581±0.003	0.673±0.002	3.908±0.016	3.196±0.123	0.217±0.009	9.303±0.089
DPO [28]	0.426±0.002	0.595±0.002	0.689±0.002	3.782±0.014	2.523±0.091	0.219±0.007	9.356±0.077

Table 1. **Preference data improves alignment.** We find that DPO performs better than RLHF. It is important to note that the FID metric is an inaccurate measure of the quality of the motion. In particular, our labelers prefer outputs from DPO over MotionGPT.

We directly train our policy with Eq. 9 on the preference dataset. Its gradient formula yields a very intuitive understanding of the optimized objective: it increases the likelihood of the preferred sample and decreases the likelihood of dispreferred samples. In formulae, each gradient step is:

$$-\beta \mathbb{E}_{\mathcal{D}} \left[w(\mathbf{x}, \mathbf{y}_w, \mathbf{y}_l) \left[\nabla_{\theta} \log \pi(\mathbf{y}_w | \mathbf{x}) - \nabla_{\theta} \log \pi(\mathbf{y}_l | \mathbf{x}) \right] \right] \quad (10)$$

where

$$w(\mathbf{x}, \mathbf{y}_w, \mathbf{y}_l) = \sigma(\hat{r}_{\theta}(\mathbf{x}, \mathbf{y}_l) - \hat{r}_{\theta}(\mathbf{x}, \mathbf{y}_w)), \quad (11)$$

is a per-sample weight [45, 46] that gives a higher weight when the reward model is wrong.

However, it is important to remember that DPO is still prone to overfitting as it also relies on the Bradley-Terry model. Moreover, DPO is limited to two points within the data, optimizing to maximize one while minimizing the other. In contrast, RLHF provides a training signal where the reward model generalizes via trial and error, thereby acquiring more information. We alleviate overfitting with a variant of DPO: Identity Preference Optimization (IPO) [3]. Specifically, IPO does not rely on the Bradley-Terry model by setting Ψ as the identity function.

5. Experiments

We organize this section as follows. First, we present details of our implementation of both methods: RLHF and DPO. Second, we present the evaluation metrics that follow standard practice in text-to-motion generation. Then, our main results show an improvement in alignment with text, compared with MotionGPT. Finally, we present ablations to understand key design choices in DPO. In particular, we find that proper regularization is important in DPO.

During all training runs, we train for 20 epochs in total and take the epoch with the best validation set performance on HumanML3D [14]. We evaluate quantitatively on the HumanML3D test set and qualitatively on our human preference test set.

Implementation Details. Our implementations of RLHF and DPO build upon TRL [39]. We implemented RLHF with separate value and policy networks because empirically, we observed greater training stability. The value

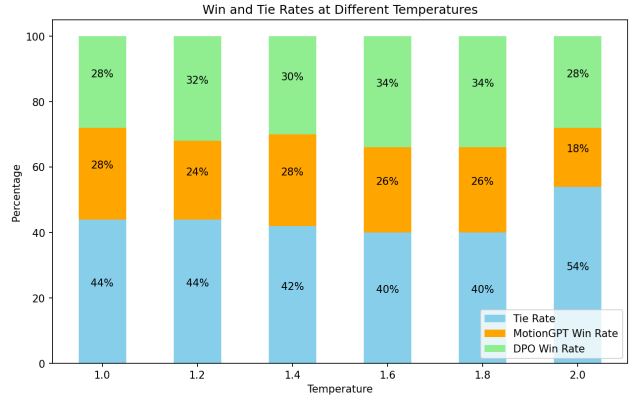


Figure 3. **Humans prefer DPO outputs over outputs from MotionGPT.** MotionGPT trained on motion data with DPO (in green) has a higher win rate. The win rate is computed on prompts never seen by the model.

network is initialized to the reward model with an additional scalar head that predicts a scalar per token (initialized with Gaussian mean 0.0 and standard deviation 0.2, bias initialized to 0.0). The policy network is initialized to the finetuned MotionGPT checkpoint¹. We remove all dropouts in the value and policy models because when dropouts are present, they cause the KL reward to be stochastic since the SFT model is stochastic. For better performance, we add reward margin (3 for “Much better,” 2 for “Better,” 1 for “Slightly better”) [36], reward whitening, and score scaling [53]. We performed a hyperparameter sweep and found that the best hyperparameters are batch size 32, learning rate 1e-5, NEFTune noise alpha 0.1 [18], fixed KL with no adaptive KL controllers, and initial KL coefficient 0.05.

For the DPO model, we initialize it to the finetuned MotionGPT checkpoint¹. We performed a hyperparameter sweep and found that the best hyperparameters are batch size 64, learning rate 1e-3, no label smoothing, PEFT [22] with LoRA [16] (rank=8, $\alpha=16$, dropout=0.05), β equal to 0.1, no dropouts in the model, and IPO loss [4].

Evaluation. We categorize popular metrics [14] in text-to-motion generation into alignment and quality. In particular, alignment is related to the alignment of the text

¹<https://huggingface.co/OpenMotionLab/MotionGPT-base>

Percent Data	Alignment				Quality		
	Top-1↑	Top-2↑	Top-3↑	MM Dist↓	MModality↑	FID↓	Diversity→
100%	0.426±0.002	0.595±0.002	0.689±0.002	3.782±0.014	2.523±0.091	0.219±0.007	9.356±0.077
80%	0.421±0.002	0.590±0.002	0.682±0.003	3.835±0.014	2.760±0.118	0.204±0.007	9.368±0.059
60%	0.417±0.002	0.585±0.002	0.677±0.002	3.872±0.011	2.594±0.100	0.233±0.008	9.334±0.070
40%	0.420±0.002	0.587±0.002	0.680±0.002	3.845±0.012	2.731±0.104	0.212±0.006	9.340±0.072
20%	0.422±0.002	0.591±0.002	0.685±0.002	3.775±0.015	2.236±0.086	0.252±0.007	9.356±0.068

Table 2. **More preference data helps.** Our analysis reveals that an increased volume of preference data enhances performance in both alignment and quality metrics, although the impact diminishes with more data. Our results demonstrate that DPO does not need a significant amount of data to exhibit performance gains.

Loss Type	Alignment				Quality		
	Top-1↑	Top-2↑	Top-3↑	MM Dist↓	MModality↑	FID↓	Diversity→
IPO [4]	0.426±0.002	0.595±0.002	0.689±0.002	3.782±0.014	2.523±0.091	0.219±0.007	9.356±0.077
KTO [10]	0.416±0.003	0.585±0.002	0.678±0.002	3.867±0.011	3.099±0.104	0.241±0.008	9.315±0.068
Hinge [28]	0.418±0.002	0.588±0.002	0.682±0.003	3.828±0.010	2.843±0.116	0.252±0.008	9.362±0.052
Sigmoid [28]	0.418±0.003	0.586±0.002	0.679±0.003	3.847±0.012	2.831±0.100	0.254±0.008	9.354±0.076

Table 3. **IPO loss performs best.** The IPO [3] variant of DPO is designed to alleviate overfitting due to the Bradley-Terry model.

prompt with the generated motion. In contrast, quality is independent of the text prompt and measures the quality of the motion. R-Precision evaluates motion-to-text retrieval accuracy based on Euclidean distances between motion sequences and text descriptions, reporting Top-1, Top-2, and Top-3 accuracies. FID measures the distribution disparity between generated and real motion using extracted motion features. MM-Dist calculates average Euclidean distances between text and generated motion features. Diversity analyzes motion variety via average Euclidean distances among randomly sampled pairs of motion. MModality generates multiple motion sequences per text description, forms pairs, and computes their average Euclidean distances.

Metrics	w/ LoRA	w/o LoRA
Top-1↑	0.426±0.002	0.394±0.001
Top-2↑	0.595±0.002	0.555±0.002
Top-3↑	0.689±0.002	0.646±0.002
MM Dist↓	3.782±0.014	4.097±0.016
MModality↑	2.523±0.091	3.285±0.114
FID↓	0.219±0.007	0.276±0.006
Diversity→	9.356±0.077	9.266±0.063

Table 4. **LoRA is an important component for preference learning.** We find that LoRA significantly contributes to the success of DPO by regularizing the model’s training.

Main results. In Tab. 1, we show our RLHF and DPO results compared to the reproduced MotionGPT baseline². Our results reveal that both RLHF and DPO outperform MotionGPT across all alignment metrics, suggesting greater alignment with text compared to the baseline. Furthermore, when considering quality metrics, RLHF and

DPO demonstrate comparable performance to MotionGPT, suggesting their efficacy in producing high-quality outputs. Notably, our findings highlight DPO’s superiority over RLHF in alignment metrics, underscoring its potential as a more effective approach for learning from preferences in text-to-motion generation tasks. Since the FID metric is not an accurate measure of the actual quality of the motion, we perform human evaluation of MotionGPT generation against DPO. We compare MotionGPT baseline generations and DPO generations at different temperatures. Given 50 random prompts taken from the test set of our preference dataset, we ask two graduate student labelers with a high agreement rate to pick which generation is the best or mark a tie if they cannot make a choice. In Fig. 3, we show the average DPO win rate, MotionGPT win rate, and tie rate. On average, DPO generations perform better than MotionGPT generations at all temperature levels, indicating not only that humans prefer DPO outputs over MotionGPT outputs, but also that its good performance is sustained at different temperature levels.

Ablation. As we have seen in Sec. 4, an important aspect of preference learning is the trade-off between optimizing the reward model and the KL regularization. Additionally, since DPO does not suffer from reward hacking and performs better than RLHF, we perform our ablation studies on our DPO baseline. First, we try different parameters that directly or indirectly improve the regularization of the reference model during training. In Fig. 5, we find that a β around 0.10 performs the best; overall, the model is robust to different choices of β , underscoring the robustness of DPO. Second, we find that IPO [3] performs best compared to other variants of the DPO loss (where sigmoid is the standard Bradley-Terry model used in the original DPO

²<https://github.com/OpenMotionLab/MotionGPT/tree/main>

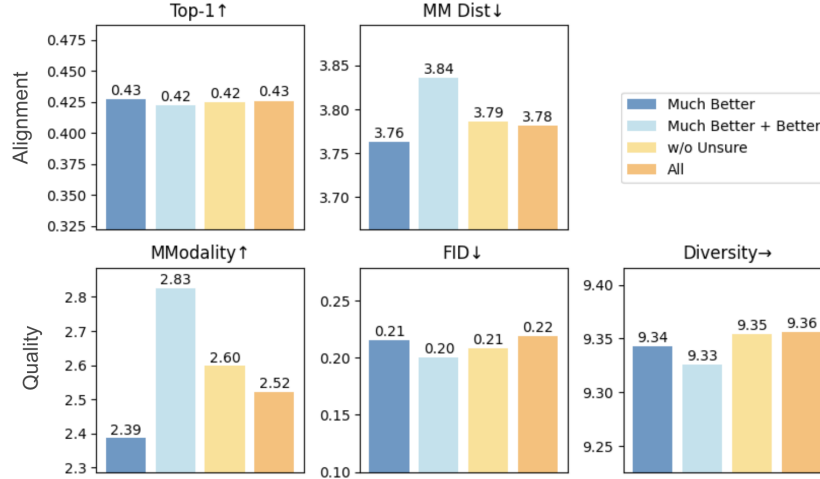


Figure 4. **Samples with preference degrees “Much better” and “Better” provide most of the performance gains.** Adding in “Slightly better” and “Negligibly better/unsure” samples slightly improves alignment but decreases quality.

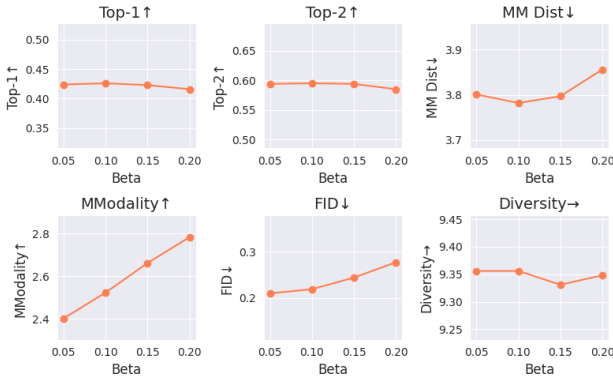


Figure 5. **Model is robust to choices of β .** Values of β increasing from 0.05 to 0.20 generally do not impact alignment.

method). As mentioned in Sec. 4, IPO was specifically designed to alleviate overfitting due to the Bradley-Terry model. Third, while LoRA was designed to reduce the cost of training, we observe that it plays an important role in regularizing the model. Tab. 4 shows significant gains from using LoRA. Finally, we study how the scale of the dataset affects training, both in terms of the quantity and the degree of preference. Tab. 2 shows that more data helps. However, we find the gains are not significant, showing that current text-to-motion generative methods do not require a significant amount of preference data to observe improvements. Additionally, in Fig. 4, we train our models on the different preference splits. We find that samples labeled as “Much better” provide most of the performance gains. Our results suggest that labelers should focus on labeling samples with a considerable visual difference.

6. Discussion

This paper is the first work that explores preference learning for text-to-human generation, *i.e.*, a cheaper supervision from human labelers for text-to-human generation. By annotating 3,528 preference pairs and introducing a degree of preference for each choice, we have laid the groundwork for more nuanced and human-like text-to-motion generation capabilities. Our pioneering efforts have shown that labelers significantly favor the outputs generated by MotionGPT when it is trained with preference data, highlighting the potential of preference learning in enhancing the alignment of generated motions across various settings.

This paper is limited to exploring preference data on MotionGPT. It would be valuable to analyze the transferability of such a dataset to other models. Additionally, we did not use the skipped samples as both samples did not generate perceptually realistic motion, while the unsure samples generated at least realistic motion. It would be interesting to see how these samples can be leveraged, for instance, with unlikelihood learning on these samples. Furthermore, prior work in image generation used a reward model trained on preference data as a metric for evaluating generation. Similarly, it would be a valuable metric for text-to-motion generation as R-precision and FID correlate poorly with human evaluation. Moreover, it would be interesting to study preference learning on bigger datasets such as Motion-X [21].

Acknowledgments

This work was supported by the Natural Science Foundation of China (U2336214, 62332019), Beijing Natural Science Foundation (L222008), and Beijing Hospitals Authority Clinical Medicine Development of special funding support (ZLRK202330).

References

- [1] Abubakar Abid, Ali Abdalla, Ali Abid, Dawood Khan, Abdulrahman Alfozan, and James Zou. Gradio: Hassle-free sharing and testing of ml models in the wild. *arXiv preprint arXiv:1906.02569*, 2019. 3
- [2] Samaneh Azadi, Akbar Shah, Thomas Hayes, Devi Parikh, and Sonal Gupta. Make-an-animation: Large-scale text-conditional 3d human motion generation, 2023. 1, 2
- [3] Mohammad Gheshlaghi Azar, Mark Rowland, Bilal Piot, Daniel Guo, Daniele Calandriello, Michal Valko, and Rémi Munos. A general theoretical paradigm to understand learning from human preferences, 2023. 4, 6, 7
- [4] Mohammad Gheshlaghi Azar, Mark Rowland, Bilal Piot, Daniel Guo, Daniele Calandriello, Michal Valko, and Rémi Munos. A general theoretical paradigm to understand learning from human preferences, 2023. 2, 6, 7
- [5] Ralph Allan Bradley and Milton E. Terry. Rank analysis of incomplete block designs: I. the method of paired comparisons. *Biometrika*, 39(3/4):324–345, 1952. 2, 5
- [6] Xin Chen, Biao Jiang, Wen Liu, Zilong Huang, Bin Fu, Tao Chen, Jingyi Yu, and Gang Yu. Executing your commands via motion diffusion in latent space, 2023. 1, 2
- [7] Zixiang Chen, Yihe Deng, Huizhuo Yuan, Kaixuan Ji, and Quanquan Gu. Self-play fine-tuning converts weak language models to strong language models, 2024. 2
- [8] Paul F Christiano, Jan Leike, Tom Brown, Miljan Martic, Shane Legg, and Dario Amodei. Deep reinforcement learning from human preferences. In *Advances in Neural Information Processing Systems*. Curran Associates, Inc., 2017. 2
- [9] Geoffrey Cideron, Sertan Girgin, Mauro Verzetti, Damien Vincent, Matej Kastelic, Zalán Borsos, Brian McWilliams, Victor Ungureanu, Olivier Bachem, Olivier Pietquin, Matthieu Geist, Léonard Hussenot, Neil Zeghidour, and Andrea Agostinelli. Musicrl: Aligning music generation to human preferences, 2024. 3
- [10] Kawin Ethayarajh, Winnie Xu, Niklas Muennighoff, Dan Jurafsky, and Douwe Kiela. Kto: Model alignment as prospect theoretic optimization, 2024. 2, 7
- [11] Deep Ganguli, Liane Lovitt, Jackson Kernion, Amanda Askell, Yuntao Bai, Saurav Kadavath, Ben Mann, Ethan Perez, Nicholas Schiefer, Kamal Ndousse, Andy Jones, Sam Bowman, Anna Chen, Tom Conerly, Nova DasSarma, Dawn Drain, Nelson Elhage, Sheer El-Showk, Stanislav Fort, Zac Hatfield-Dodds, Tom Henighan, Danny Hernandez, Tristan Hume, Josh Jacobson, Scott Johnston, Shauna Kravec, Catherine Olsson, Sam Ringer, Eli Tran-Johnson, Dario Amodei, Tom Brown, Nicholas Joseph, Sam McCandlish, Chris Olah, Jared Kaplan, and Jack Clark. Red teaming language models to reduce harms: Methods, scaling behaviors, and lessons learned, 2022. 2
- [12] Kehong Gong, Dongze Lian, Heng Chang, Chuan Guo, Zihang Jiang, Xinxin Zuo, Michael Bi Mi, and Xinchao Wang. Tm2d: Bimodality driven 3d dance generation via music-text integration. In *Proceedings of the IEEE/CVF International Conference on Computer Vision (ICCV)*, pages 9942–9952, 2023. 1, 2
- [13] Caglar Gulcehre, Tom Le Paine, Srivatsan Srinivasan, Ksenia Konyushkova, Lotte Weerts, Abhishek Sharma, Aditya Siddhant, Alex Ahern, Miaosen Wang, Chenjie Gu, Wolfgang Macherey, Arnaud Doucet, Orhan Firat, and Nando de Freitas. Reinforced self-training (rest) for language modeling, 2023. 2
- [14] Chuan Guo, Shihao Zou, Xinxin Zuo, Sen Wang, Wei Ji, Xingyu Li, and Li Cheng. Generating diverse and natural 3d human motions from text. In *Proceedings of the IEEE/CVF Conference on Computer Vision and Pattern Recognition (CVPR)*, pages 5152–5161, 2022. 6
- [15] Chuan Guo, Xinxin Zuo, Sen Wang, and Li Cheng. Tm2t: Stochastic and tokenized modeling for the reciprocal generation of 3d human motions and texts. In *ECCV*, 2022. 1, 2
- [16] Edward J Hu, Yelong Shen, Phillip Wallis, Zeyuan Allen-Zhu, Yanzhi Li, Shean Wang, Lu Wang, and Weizhu Chen. LoRA: Low-rank adaptation of large language models. In *International Conference on Learning Representations*, 2022. 6
- [17] Borja Ibarz, Jan Leike, Tobias Pohlen, Geoffrey Irving, Shane Legg, and Dario Amodei. Reward learning from human preferences and demonstrations in atari. In *Advances in Neural Information Processing Systems*. Curran Associates, Inc., 2018. 2
- [18] Neel Jain, Ping yeh Chiang, Yuxin Wen, John Kirchenbauer, Hong-Min Chu, Gowthami Somepalli, Brian R. Bartoldson, Bhavya Kailkhura, Avi Schwarzschild, Aniruddha Saha, Micah Goldblum, Jonas Geiping, and Tom Goldstein. NEFTune: Noisy embeddings improve instruction finetuning. In *The Twelfth International Conference on Learning Representations*, 2024. 6
- [19] Biao Jiang, Xin Chen, Wen Liu, Jingyi Yu, Gang Yu, and Tao Chen. Motiongpt: Human motion as a foreign language. *arXiv preprint arXiv:2306.14795*, 2023. 1, 2, 3, 6
- [20] Kimin Lee, Hao Liu, Moonkyung Ryu, Olivia Watkins, Yuqing Du, Craig Boutilier, Pieter Abbeel, Mohammad Ghavamzadeh, and Shixiang Shane Gu. Aligning text-to-image models using human feedback, 2023. 2
- [21] Jing Lin, Ailing Zeng, Shunlin Lu, Yuanhao Cai, Ruimao Zhang, Haoqian Wang, and Lei Zhang. Motion-x: A large-scale 3d expressive whole-body human motion dataset. *Advances in Neural Information Processing Systems*, 2023. 1, 8
- [22] Sourab Mangrulkar, Sylvain Gugger, Lysandre Debut, Younes Belkada, Sayak Paul, and Benjamin Bossan. Peft: State-of-the-art parameter-efficient fine-tuning methods. <https://github.com/huggingface/peft>, 2022. 6
- [23] Jacob Menick, Maja Trebacz, Vladimir Mikulik, John Aslanides, Francis Song, Martin Chadwick, Mia Glaese, Susannah Young, Lucy Campbell-Gillingham, Geoffrey Irving, and Nat McAleese. Teaching language models to support answers with verified quotes, 2022. 2
- [24] Reiichiro Nakano, Jacob Hilton, Suchir Balaji, Jeff Wu, Long Ouyang, Christina Kim, Christopher Hesse, Shantanu Jain, Vineet Kosaraju, William Saunders, Xu Jiang,

Karl Cobbe, Tyna Eloundou, Gretchen Krueger, Kevin Button, Matthew Knight, Benjamin Chess, and John Schulman. Webgpt: Browser-assisted question-answering with human feedback, 2022. [2](#)

- [25] OpenAI, :, Josh Achiam, Steven Adler, Sandhini Agarwal, Lama Ahmad, Ilge Akkaya, Florencia Leoni Aleman, Diogo Almeida, Janko Altschmidt, Sam Altman, Shyamal Anadkat, Red Avila, Igor Babuschkin, Suchir Balaji, Valerie Balcom, Paul Baltescu, Haiming Bao, Mo Bavarian, Jeff Belgum, Irwan Bello, Jake Berdine, Gabriel Bernadett-Shapiro, Christopher Berner, Lenny Bogdonoff, Oleg Boiko, Madeleine Boyd, Anna-Luisa Brakman, Greg Brockman, Tim Brooks, Miles Brundage, Kevin Button, Trevor Cai, Rosie Campbell, Andrew Cann, Brittany Carey, Chelsea Carlson, Rory Carmichael, Brooke Chan, Che Chang, Fotis Chantzis, Derek Chen, Sully Chen, Ruby Chen, Jason Chen, Mark Chen, Ben Chess, Chester Cho, Casey Chu, Hyung Won Chung, Dave Cummings, Jeremiah Currier, Yunxing Dai, Cory Decareaux, Thomas Degry, Noah Deutsch, Damien Deville, Arka Dhar, David Dohan, Steve Dowling, Sheila Dunning, Adrien Ecoffet, Atty Eleti, Tyna Eloundou, David Farhi, Liam Fedus, Niko Felix, Simón Posada Fishman, Juston Forte, Isabella Fulford, Leo Gao, Elie Georges, Christian Gibson, Vik Goel, Tarun Gogineni, Gabriel Goh, Rapha Gontijo-Lopes, Jonathan Gordon, Morgan Grafstein, Scott Gray, Ryan Greene, Joshua Gross, Shixiang Shane Gu, Yufei Guo, Chris Hallacy, Jesse Han, Jeff Harris, Yuchen He, Mike Heaton, Johannes Heidecke, Chris Hesse, Alan Hickey, Wade Hickey, Peter Hoeschele, Brandon Houghton, Kenny Hsu, Shengli Hu, Xin Hu, Joost Huizinga, Shantanu Jain, Shawn Jain, Joanne Jang, Angela Jiang, Roger Jiang, Haozhun Jin, Denny Jin, Shino Jomoto, Billie Jonn, Heewoo Jun, Tomer Kaftan, Łukasz Kaiser, Ali Kamali, Ingmar Kanitscheider, Nitish Shirish Keskar, Tabarak Khan, Logan Kilpatrick, Jong Wook Kim, Christina Kim, Yongjik Kim, Hendrik Kirchner, Jamie Kiros, Matt Knight, Daniel Kokotajlo, Łukasz Kondraciuk, Andrew Kondrich, Aris Konstantinidis, Kyle Kopic, Gretchen Krueger, Vishal Kuo, Michael Lampe, Ikai Lan, Teddy Lee, Jan Leike, Jade Leung, Daniel Levy, Chak Ming Li, Rachel Lim, Molly Lin, Stephanie Lin, Mateusz Litwin, Theresa Lopez, Ryan Lowe, Patricia Lue, Anna Makanju, Kim Malfacini, Sam Manning, Todor Markov, Yaniv Markovski, Bianca Martin, Katie Mayer, Andrew Mayne, Bob McGrew, Scott Mayer McKinney, Christine McLeavey, Paul McMillan, Jake McNeil, David Medina, Aalok Mehta, Jacob Menick, Luke Metz, Andrey Mishchenko, Pamela Mishkin, Vinnie Monaco, Evan Morikawa, Daniel Mossing, Tong Mu, Mira Murati, Oleg Murk, David Mély, Ashvin Nair, Reiichiro Nakano, Rajeev Nayak, Arvind Neelakantan, Richard Ngo, Hyeonwoo Noh, Long Ouyang, Cullen O’Keefe, Jakub Pachocki, Alex Paino, Joe Palermo, Ashley Pantuliano, Giambattista Parascandolo, Joel Parish, Emy Parparita, Alex Passos, Mikhail Pavlov, Andrew Peng, Adam Perelman, Filipe de Avila Belbute Peres, Michael Petrov, Henrique Ponde de Oliveira Pinto, Michael, Pokorny, Michelle Pokrass, Vitchyr Pong, Tolly Powell, Alethea Power, Boris Power, Elizabeth Proehl, Raul Puri, Alec Radford, Jack Rae, Aditya Ramesh, Cameron Raymond, Francis Real, Kendra Rimbach, Carl Ross, Bob Rotsted, Henri Roussez, Nick Ryder, Mario Saltarelli, Ted Sanders, Shibani Santurkar, Girish Sasstry, Heather Schmidt, David Schnurr, John Schulman, Daniel Selsam, Kyla Sheppard, Toki Sherbakov, Jessica Shieh, Sarah Shoker, Pranav Shyam, Szymon Sidor, Eric Sigler, Maddie Simens, Jordan Sitkin, Katarina Slama, Ian Sohl, Benjamin Sokolowsky, Yang Song, Natalie Staudacher, Felipe Petroski Such, Natalie Summers, Ilya Sutskever, Jie Tang, Nikolas Tezak, Madeleine Thompson, Phil Tillet, Amin Tootoonchian, Elizabeth Tseng, Preston Tuggle, Nick Turley, Jerry Tworek, Juan Felipe Cerón Uribe, Andrea Vallone, Arun Vijayvergiya, Chelsea Voss, Carroll Wainwright, Justin Jay Wang, Alvin Wang, Ben Wang, Jonathan Ward, Jason Wei, CJ Weinmann, Akila Welihinda, Peter Welinder, Jiayi Weng, Lilian Weng, Matt Wiethoff, Dave Willner, Clemens Winter, Samuel Wolrich, Hannah Wong, Lauren Workman, Sherwin Wu, Jeff Wu, Michael Wu, Kai Xiao, Tao Xu, Sarah Yoo, Kevin Yu, Qiming Yuan, Wojciech Zaremba, Rowan Zellers, Chong Zhang, Marvin Zhang, Shengjia Zhao, Tianhao Zheng, Juntang Zhuang, William Zhuk, and Barret Zoph. Gpt-4 technical report, 2023. [2](#), [3](#)
- [26] Long Ouyang, Jeffrey Wu, Xu Jiang, Diogo Almeida, Carroll Wainwright, Pamela Mishkin, Chong Zhang, Sandhini Agarwal, Katarina Slama, Alex Ray, John Schulman, Jacob Hilton, Fraser Kelton, Luke Miller, Maddie Simens, Amanda Askell, Peter Welinder, Paul F Christiano, Jan Leike, and Ryan Lowe. Training language models to follow instructions with human feedback. In *Advances in Neural Information Processing Systems*, pages 27730–27744. Curran Associates, Inc., 2022. [1](#), [2](#), [6](#)
- [27] Sigal Raab, Inbal Leibovitch, Guy Tevet, Moab Arar, Amit H. Bermano, and Daniel Cohen-Or. Single motion diffusion, 2023. [1](#), [2](#)
- [28] Rafael Rafailov, Archit Sharma, Eric Mitchell, Christopher D Manning, Stefano Ermon, and Chelsea Finn. Direct preference optimization: Your language model is secretly a reward model. In *Advances in Neural Information Processing Systems*, pages 53728–53741. Curran Associates, Inc., 2023. [2](#), [6](#), [7](#)
- [29] Colin Raffel, Noam Shazeer, Adam Roberts, Katherine Lee, Sharan Narang, Michael Matena, Yanqi Zhou, Wei Li, and Peter J. Liu. Exploring the limits of transfer learning with a unified text-to-text transformer, 2020. [2](#)
- [30] Yonatan Shafir, Guy Tevet, Roy Kapon, and Amit H. Bermano. Human motion diffusion as a generative prior, 2023. [1](#), [2](#)
- [31] Zhihong Shao, Peiyi Wang, Qihao Zhu, Runxin Xu, Junxiao Song, Mingchuan Zhang, Y. K. Li, Y. Wu, and Daya Guo. Deepseekmath: Pushing the limits of mathematical reasoning in open language models, 2024. [2](#)
- [32] Nisan Stiennon, Long Ouyang, Jeffrey Wu, Daniel Ziegler, Ryan Lowe, Chelsea Voss, Alec Radford, Dario Amodei, and Paul F Christiano. Learning to summarize with human feedback. In *Advances in Neural Information Processing Systems*, pages 3008–3021. Curran Associates, Inc., 2020. [1](#), [2](#)

- [33] Guy Tevet, Sigal Raab, Brian Gordon, Yonatan Shafir, Amit H Bermano, and Daniel Cohen-Or. Human motion diffusion model. *arXiv preprint arXiv:2209.14916*, 2022. 1, 2
- [34] Romal Thoppilan, Daniel De Freitas, Jamie Hall, Noam Shazeer, Apoorv Kulshreshtha, Heng-Tze Cheng, Alicia Jin, Taylor Bos, Leslie Baker, Yu Du, YaGuang Li, Hongrae Lee, Huaixiu Steven Zheng, Amin Ghafouri, Marcelo Menegali, Yanping Huang, Maxim Krikun, Dmitry Lepikhin, James Qin, Dehao Chen, Yuanzhong Xu, Zhifeng Chen, Adam Roberts, Maarten Bosma, Vincent Zhao, Yanqi Zhou, Chung-Ching Chang, Igor Krivokon, Will Rusch, Marc Pickett, Pranesh Srinivasan, Laichee Man, Kathleen Meier-Hellstern, Meredith Ringel Morris, Tulsee Doshi, Renelito Delos Santos, Toju Duke, Johnny Soraker, Ben Zevenbergen, Vinodkumar Prabhakaran, Mark Diaz, Ben Hutchinson, Kristen Olson, Alejandra Molina, Erin Hoffman-John, Josh Lee, Lora Aroyo, Ravi Rajakumar, Alena Butryna, Matthew Lamm, Viktoriya Kuzmina, Joe Fenton, Aaron Cohen, Rachel Bernstein, Ray Kurzweil, Blaise Aguera-Arcas, Claire Cui, Marian Croak, Ed Chi, and Quoc Le. Lambda: Language models for dialog applications, 2022. 2
- [35] Hugo Touvron, Thibaut Lavril, Gautier Izacard, Xavier Martinet, Marie-Anne Lachaux, Timothée Lacroix, Baptiste Rozière, Naman Goyal, Eric Hambro, Faisal Azhar, Aurelien Rodriguez, Armand Joulin, Edouard Grave, and Guillaume Lample. Llama: Open and efficient foundation language models, 2023. 2
- [36] Hugo Touvron, Louis Martin, Kevin Stone, Peter Albert, Amjad Almahairi, Yasmine Babaei, Nikolay Bashlykov, Soumya Batra, Prajjwal Bhargava, Shriti Bhosale, Dan Bikel, Lukas Blecher, Cristian Canton Ferrer, Moya Chen, Guillem Cucurull, David Esiobu, Jude Fernandes, Jeremy Fu, Wenyin Fu, Brian Fuller, Cynthia Gao, Vedanuj Goswami, Naman Goyal, Anthony Hartshorn, Saghar Hosseini, Rui Hou, Hakan Inan, Marcin Kardas, Viktor Kerkez, Madian Khabsa, Isabel Kloumann, Artem Korenev, Punit Singh Koura, Marie-Anne Lachaux, Thibaut Lavril, Jenya Lee, Diana Liskovich, Yinghai Lu, Yuning Mao, Xavier Martinet, Todor Mihaylov, Pushkar Mishra, Igor Molybog, Yixin Nie, Andrew Poulton, Jeremy Reizenstein, Rashi Rungta, Kalyan Saladi, Alan Schelten, Ruan Silva, Eric Michael Smith, Ranjan Subramanian, Xiaoqing Ellen Tan, Binh Tang, Ross Taylor, Adina Williams, Jian Xiang Kuan, Puxin Xu, Zheng Yan, Iliyan Zarov, Yuchen Zhang, Angela Fan, Melanie Kambadur, Sharan Narang, Aurelien Rodriguez, Robert Stojnic, Sergey Edunov, and Thomas Scialom. Llama 2: Open foundation and finetuned chat models, 2023. 1, 2, 6
- [37] Aaron van den Oord, Oriol Vinyals, and koray kavukcuoglu. Neural discrete representation learning. In *Advances in Neural Information Processing Systems*. Curran Associates, Inc., 2017. 2, 3
- [38] Ashish Vaswani, Noam Shazeer, Niki Parmar, Jakob Uszkoreit, Llion Jones, Aidan N Gomez, Łukasz Kaiser, and Illia Polosukhin. Attention is all you need. In *Advances in Neural Information Processing Systems*. Curran Associates, Inc., 2017. 2
- [39] Leandro von Werra, Younes Belkada, Lewis Tunstall, Edward Beeching, Tristan Thrush, Nathan Lambert, and Shengyi Huang. Trl: Transformer reinforcement learning. <https://github.com/huggingface/trl>, 2020. 6
- [40] Binghai Wang, Rui Zheng, Lu Chen, Yan Liu, Shihan Dou, Caishuang Huang, Wei Shen, Senjie Jin, Enyu Zhou, Chenyu Shi, Songyang Gao, Nuo Xu, Yuhao Zhou, Xiaoran Fan, Zhiheng Xi, Jun Zhao, Xiao Wang, Tao Ji, Hang Yan, Lixing Shen, Zhan Chen, Tao Gui, Qi Zhang, Xipeng Qiu, Xuanjing Huang, Zuxuan Wu, and Yu-Gang Jiang. Secrets of rlhf in large language models part ii: Reward modeling, 2024. 1
- [41] Zilin Wang, Haolin Zhuang, Lu Li, Yinmin Zhang, Junjie Zhong, Jun Chen, Yu Yang, Boshi Tang, and Zhiyong Wu. Explore 3d dance generation via reward model from automatically-ranked demonstrations. In *AAAI*, 2024. 1
- [42] Xiaoshi Wu, Keqiang Sun, Feng Zhu, Rui Zhao, and Hongsheng Li. Better aligning text-to-image models with human preference, 2023. 2
- [43] Hongyi Yuan, Zheng Yuan, Chuanqi Tan, Wei Wang, Songfang Huang, and Fei Huang. Rrhf: Rank responses to align language models with human feedback. In *Advances in Neural Information Processing Systems*, pages 10935–10950. Curran Associates, Inc., 2023. 2
- [44] Ye Yuan, Jiaming Song, Umar Iqbal, Arash Vahdat, and Jan Kautz. Physdiff: Physics-guided human motion diffusion model, 2022. 1, 2
- [45] Yang Yue, Bingyi Kang, Xiao Ma, Zhongwen Xu, Gao Huang, and Shuicheng Yan. Boosting offline reinforcement learning via data rebalancing. *NIPS RL Workshop*, 2022. 6
- [46] Yang Yue, Bingyi Kang, Xiao Ma, Gao Huang, Shiji Song, and Shuicheng Yan. Offline prioritized experience replay. *arXiv preprint arXiv:2306.05412*, 2023. 6
- [47] Jianrong Zhang, Yangsong Zhang, Xiaodong Cun, Shaoli Huang, Yong Zhang, Hongwei Zhao, Hongtao Lu, and Xi Shen. T2m-gpt: Generating human motion from textual descriptions with discrete representations, 2023. 1, 2
- [48] Mingyuan Zhang, Zhongang Cai, Liang Pan, Fangzhou Hong, Xinying Guo, Lei Yang, and Ziwei Liu. Motiondiffuse: Text-driven human motion generation with diffusion model. *arXiv preprint arXiv:2208.15001*, 2022. 2
- [49] Mingyuan Zhang, Xinying Guo, Liang Pan, Zhongang Cai, Fangzhou Hong, Huirong Li, Lei Yang, and Ziwei Liu. Remodiffuse: Retrieval-augmented motion diffusion model, 2023.
- [50] Qincheng Zhang, Jiaming Song, Xun Huang, Yongxin Chen, and Mingyu Liu. Diffcollage: Parallel generation of large content with diffusion models. In *CVPR*, 2023. 2
- [51] Yaqi Zhang, Di Huang, Bin Liu, Shixiang Tang, Yan Lu, Lu Chen, Lei Bai, Qi Chu, Nenghai Yu, and Wanli Ouyang. Motiongpt: Finetuned llms are general-purpose motion generators. *arXiv preprint arXiv:2306.10900*, 2023. 1, 2
- [52] Yao Zhao, Rishabh Joshi, Tianqi Liu, Misha Khalman, Mohammad Saleh, and Peter J. Liu. Slic-hf: Sequence likelihood calibration with human feedback, 2023. 2

- [53] Rui Zheng, Shihan Dou, Songyang Gao, Yuan Hua, Wei Shen, Binghai Wang, Yan Liu, Senjie Jin, Qin Liu, Yuhao Zhou, Limao Xiong, Lu Chen, Zhiheng Xi, Nuo Xu, Wenbin Lai, Minghao Zhu, Cheng Chang, Zhangyue Yin, Rongxiang Weng, Wensen Cheng, Haoran Huang, Tianxiang Sun, Hang Yan, Tao Gui, Qi Zhang, Xipeng Qiu, and Xuanjing Huang. Secrets of rlhf in large language models part i: Ppo, 2023. [1](#), [6](#)
- [54] Daniel M. Ziegler, Nisan Stiennon, Jeffrey Wu, Tom B. Brown, Alec Radford, Dario Amodei, Paul Christiano, and Geoffrey Irving. Fine-tuning language models from human preferences. *arXiv preprint arXiv:1909.08593*, 2019. [1](#), [2](#)